Satellite, UAV, and Geophysical Data to Surface and Subsurface Imaging of Geographically Isolated Wetlands at the Atlantic Forest-Cerrado Interface of Brazil.

Lucas Moreira Furlan*[1], Manuel Eduardo Ferreira[2], César Augusto Moreira[1], Paulo Guilherme de Alencar[1], Matheus Felipe Stanfoca Casagrande[1], Vania Rosolen[1]. [1]Unesp, [2]UGF.

This paper was prepared for presentation during the 18th International Congress of the Brazilian Geophysical Society held in Rio de Janeiro, Brazil, 16-19 October 2023.

Abstract

This study focuses on evaluating the use of multisource remote sensing datasets to assess the hydrodynamics of small isolated wetlands in the Atlantic Forest and Brazilian savanna interface in São Paulo State, Brazil. The study involved pixel-based supervised classification using Landsat and CBERS satellite data, aerial images acquired from a UAV, 2D and 3D Electrical Resistivity Tomography (ERT) data, and climatological data analysis. The results allowed the classification of the ecosystems as geographically isolated wetlands (GIWs) and revealed spatial variations in waterlogged areas, vegetation patterns, soil-water interaction, and direct aquifer recharge. The findings provide valuable insights for accurately characterizing the hydrodynamics and hydroperiods of small wetlands at a local scale, aiding in their understanding, monitoring, and restoration.

Introduction

The integration of remote sensing and near-surface geophysics provides valuable information for understanding and addressing hydrological uncertainties in natural wetlands (Mousa et al., 2022; Mitsch and Grosselink., 2000). Wetlands play a crucial role in the hydrology of catchments, and remote sensing is a powerful tool for mapping wetland location, measuring water flow and storage, and assessing connectivity between water bodies. Various sensors, such as optical, active microwave, passive microwave, thermal, and gravimetry, have been used in wetland studies (Kandus et al., 2018).

Unmanned aerial vehicles (UAVs or drones) have emerged as advanced tools for collecting high-resolution data in time and space, particularly for managing catchments and addressing water-related issues. UAVs complement satellite systems by providing very high-resolution image acquisition and unlimited temporal coverage, making them suitable for small enclosed areas with high seasonal dynamics.

Assessing the hydrological status of small isolated wetlands requires integrating data from surface water, regolith, and groundwater. Near-surface geophysics, specifically Electrical Resistivity Tomography (ERT), offers reliable images of the shallow subsurface (Rubin, 2006; Moreira et al., 2021). ERT is suitable for hydrogeological studies as it provides subsurface imaging at intermediate scales, capturing variations in electrical properties related to different materials and levels of wetness or water saturation.

The challenge lies in integrating geoinformation from remote sensing and geophysical measurements into a consistent model that represents the Earth's Critical Zone, requiring spatially distributed data of both surface and subsurface properties.

The aim of this study is to propose a hydrodynamic model for small isolated wetlands based on the physical imaging response obtained from multiple remote sensing technologies, including satellites, UAVs, and ERT. The motivation behind this research is the increasing concern about water quality and availability in the São Paulo State countryside, which is located between the Atlantic Forest and Cerrado biomes (Figure 1). Factors such as prolonged dry seasons, population growth, water-dependent economic activities, and land use conversion for sugarcane agriculture have led to water scarcity, making the region critical in terms of water resources.

Figure 1. Study area: The Corumbataí River Basin.

Method

To identify the small isolated wetlands, hydrogeomorphological features were used, including circular or oval shapes, depressed areas surrounded by uplands, the absence of visible surface channels connecting to rivers, and the presence of vegetation (grasses) typical of hydromorphic soils. Two wetlands, referred to as Wetland A and Wetland B, were selected for the study. They are located close to each other, approximately 1.5 km apart, and have specific coordinates (latitude, longitude, and altitude).

The imaging methodology approaches the satellite and UAV (Figure 2), in order to compose a sequence of multisource and multi-scale studies covering the identification, classification, delineation and acquisition of qualitative and quantitative data.

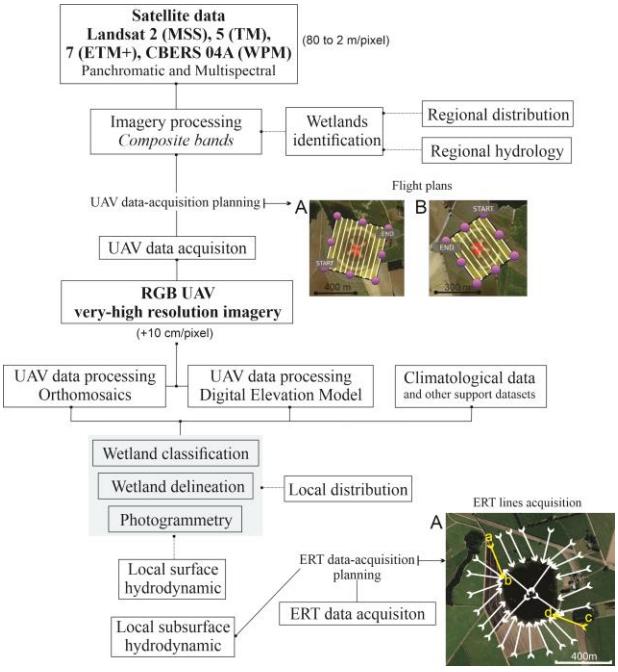

Figure 2. Multi-scale process used during the development of the different stages of the study.

Satellite images acquisition and bands composition

Satellite data was used to determine the location of the wetlands within the catchment and to characterize their hydroperiod. Images from different sensors and bands of Landsat (USGS-NASA) and CBERS-04A (China-Brazil Earth Resources Satellite) satellites were acquired free of charge. The data covered the period from 1975 to 2020 and were obtained from the platform of the National Institute for Space Research and the USGS Earth Explorer platform.

UAV data acquisition and processing

The DJI Phantom 4 Pro UAV equipped with a DJI 1" CMOS sensor with 20 megapixels, covering RGB bands, was used for data collection. Flight plans were created using PIX4D software, specifying variables such as flight height, image capture interval, number of images, direction, camera angle, and flight strips. The flights were conducted over a year in two wetlands, with monthly captures except for slight variations due to weather conditions. A total of 12 orthomosaics and 2 digital elevation models were generated for each wetland. Image processing was performed using the SfM-MVS methodology with Agisoft Metashape software, including planialtimetric correction using ground control points (GCPs) and a Differential GPS (DGPS). The ground resolution achieved after GCPs correction was 3.44 cm/pixel (October 2019) and 3.48 cm/pixel (February 2020), as indicated by the processing report.

Water balance for hydrodynamic analysis

The study calculated surplus and deficit of atmospheric humidity in dry and wet seasons to validate spectral signatures used for assessing hydroperiod and wetland area. Precipitation and evapotranspiration data were obtained from a meteorological station for the corresponding months of image acquisition. The water balance was calculated using the equation WB = P - ET, where WB represents water balance in millimeters, P represents precipitation in millimeters, and ET represents reference evapotranspiration in millimeters (Fries et al., 2020).

ERT geophysical data acquisition and processing

Electrical Resistivity Tomography (ERT) is a valuable technique for shallow analysis, providing information about the subsurface's electrical resistivity based on induced electrical currents. By measuring the variability of current propagation, ERT can reveal differences in physical-chemical properties and moisture content (Kearey and Brooks, 2002; Milson, 2003). The collected data is initially known as apparent resistivity and is interpolated to create 2D sections and a 3D block model of the subsurface. The data acquisition involved 27 lines (200 m length) covering wetland A during both wet and dry seasons, using the Terrameter LS equipment. Its specifications are the following: 84 channels, 250 W, a maximum current of 2.5 A, and 1 mV resolution (ABEM, 2012).
The data processing was performed using Res2Dinv software, employing the Ordinary Least Squares (OLS) mathematical model for interpolation and inversion. The final 3D block model was created in the Oasis Montaj platform, allowing visualization of the subsurface at different depths.

Results

The analysis of satellite images using pixel contrast allowed for the grouping of Land Use Land Cover (LULC) categories based on the varying hues and tones of soil-vegetation types and conditions. The dark color scale in the images indicated different levels of soil moisture, with water displaying strong infrared absorption. A pixel-based supervised classification was conducted, resulting in four LULC classes: Soil, Tree vegetation, Agriculture (mainly sugarcane crops), and Water. Wetland A, which experiences permanent flooding, was analyzed effectively over a 36-year period. The size of Wetland A decreased from 175,909 m² in 1984 to 149,750 m² in 2020 (Figure 3). However, accurate area calculations based on flooding were challenging for Wetland B due to its smaller size and significant seasonal hydro-variation. Wetland B also experienced the expansion of grassy and shrubby areas along its borders due to the retraction of flooding.

The hydrology of wetlands is influenced by various factors, including surface hydrology, groundwater dynamics, and the relationship between precipitation, evapotranspiration, soil water storage, and surface runoff. Understanding the processes and interactions within wetland areas, particularly regarding soil-water interaction, is complex. However, in order to assess seasonal impacts and predict potential changes in land use and climate, precipitation is considered the only source of water input, while evapotranspiration is quantified as water loss. It is important to note that there have been no reports or observations of water extraction

from the wetlands for human activities such as irrigation. In general, periods with evapotranspiration exceeding precipitation are classified as arid or dry, indicating a deficit or negative water balance, while periods with precipitation exceeding evapotranspiration are classified as humid or wet, indicating a surplus or positive water balance. The water balance graph serves as a basis for comparison with the orthomosaics generated from the data.

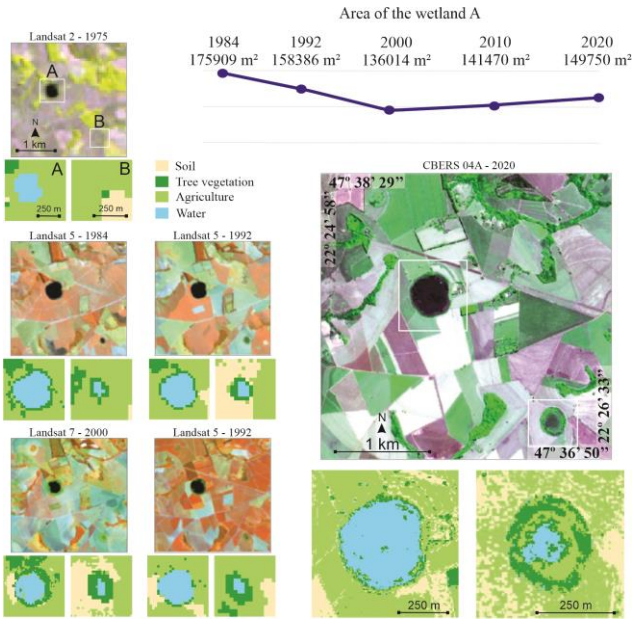

Figure 3. 1975-2020 band composition images of the Landsat series and CBERS-04A satellite. Pixel-based supervised classification in wetland A and B (zoom-in) - the wetlands chosen to be classified and monitored. The graph "Area of the wetland A" displays the result of calculations of the waterlogged area (water class) for each year-dataset, based on the supervised classifications.

The October 2019 orthomosaics, digital elevation models, and elevation profiles provide insights into the characteristics of wetlands A and B. Wetland A has perennial flooding and lacks tree vegetation, with a perimeter of 1485.1 meters. Wetland B, on the other hand, experiences temporary flooding and has tree vegetation along its boundaries, with a perimeter of 972.3 meters. Wetland A is approximately 34% larger than wetland B. In the dry-season images of wetland A, there are noticeable contrasts between dry and wet soil. Additionally, a zoomed-in portion shows water storage areas and native grasses that are tolerant to flooding. The border of wetland A exhibits soil fissures, and a closer look reveals sediment deposition within the wetland, indicating a silting process (Figure 4).

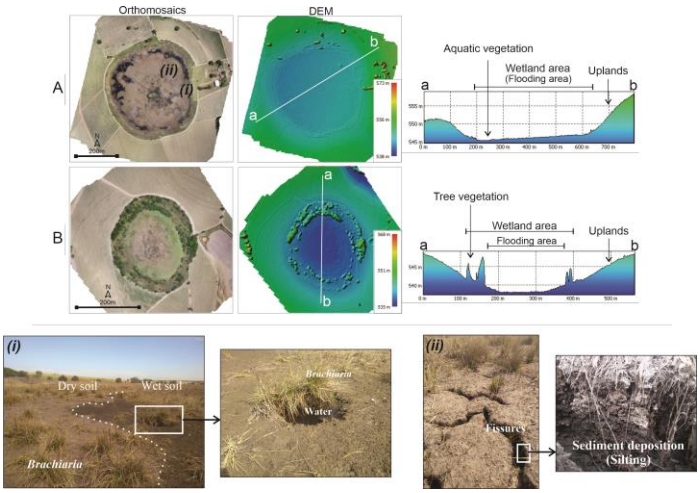

Figure 4. October-2019 orthomosaics, digital elevation models and elevation profiles (a-b) of the two wetlands A and B.

The hydrogeological interpretation of wetland A was conducted using ERT 2D inversion resistivity models, showcasing the water flow pattern and groundwater dynamics. The models illustrate a vertical downward water flow into hydric soils, reaching the shallow groundwater, which is retained by a thick horizontal argillic layer (bedrock). Two examples of the 2D inversion models are shown in Figure 8: one representing the acquisition from the hillslope to the wetland border, and the other acquired from the center to the border within the flooding area. In the first model, a high electrical resistivity (>800 Ω.m) is observed throughout the surface portion, indicating an impermeable horizontal layer approximately 30 meters thick.

This layer corresponds to the geological-stratigraphic substrate of the area, known as the Corumbataí Formation. The deep aquifer does not directly interact with surface water in the surrounding of the wetland, and its recharge and maintenance occur horizontally from a depth of 30 meters. The second model demonstrates the response of the wetland center, where the electrical resistivity is low (<20 Ω.m). This region represents the genuine interaction between surface water and groundwater. By creating a 3D block, slices were cut at different depths to observe the behavior of electrical resistivity and understand the water infiltration architecture.

The slices at various depths revealed that the central portion of the wetland becomes progressively less resistive, indicating a preferential channel for water infiltration into the deeper aquifer (Figure 5). The 35-meter depth slice displayed a horizontal distribution of zones with low electrical resistivity, indicating the horizontal recharge of the aquifer, which is also depicted in the 2D profile.

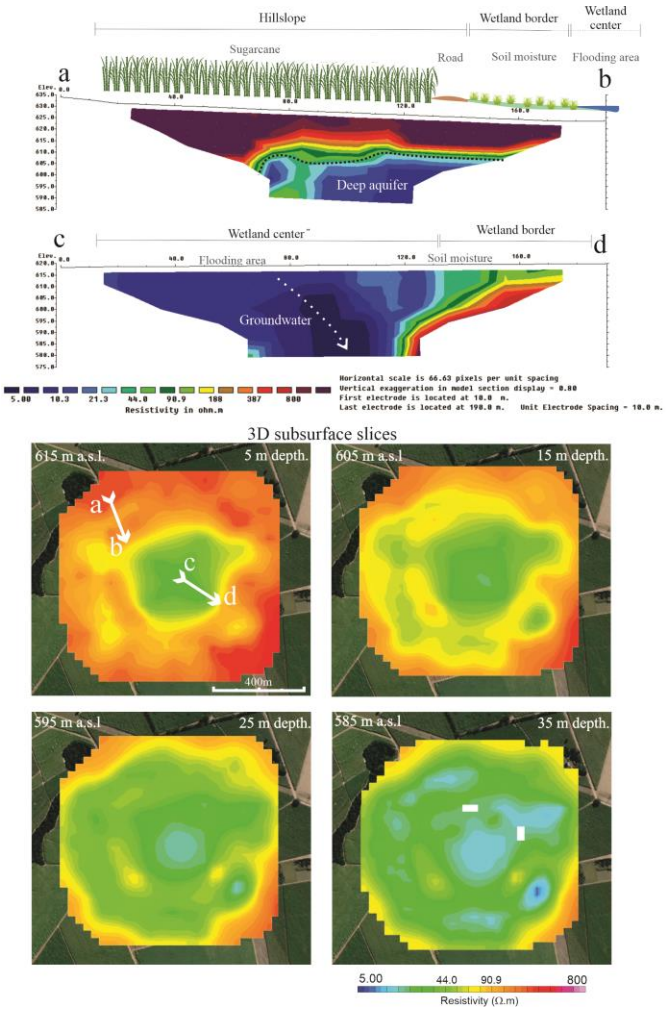

Figure 5. (a-b; c-d) 2D Inversion resistivity models, acquired based on Schlumberger array; 3D subsurface slices - visualization models, slices of the 3D blocks, resulted of lateral interpolation of 2D inversion models. Depth of 5, 15, 25 and 35 meters.

In both wetlands A and B, soil moisture and water storage are closely related to the local depressed topography in the catchments, which are geographically isolated wetlands (GIWs). The size of the wetlands varies with the seasons and is determined by the amount of water stored in the topographic depressions. Sediments deposited inside the wetlands from runoff contribute to reducing water levels and expanding the border area prone to wetness. Wetland A has experienced a significant decrease in endemic vegetation due to land-use intensification, hydrologic variability, and impacts from fire and climate changes.

The border of the wetlands, as mapped by satellite images, provides effective discrimination between water and dry soil. However, high-resolution images from unmanned aerial vehicles (UAV) are more effective in calibrating the hydrological response of the wetlands, especially when combined with climatic parameters. The wetlands' hydrodynamic and connectivity within the landscape can be traced using these visual tools, which are crucial for monitoring and managing land use and water conservation.

Human disturbance over the years has impacted the wetlands, resulting in smaller wetland areas compared to the 1970s. The wetland borders are vulnerable to erosion and sedimentation, with mineral sediments covering the organic matter accumulated on the soil surface. Changes in the volume and precipitation regime due to global climate changes can affect the wetlands' hydro-ecological functions. The difference in hydroperiods between wetlands suggests that water storage is dependent not only on precipitation, temperature, and evapotranspiration but also on the wetland's soil attributes.

The combination of UAV and electrical resistivity tomography (ERT) images is crucial for understanding the interactions between surface and subsurface water in the wetlands. UAV orthomosaics provide fine-resolution spatial data on soil moisture and water volume, while ERT helps understand subsurface water flow. These approaches enable monitoring the hydrological status of the wetlands in the catchment.

The difference in flooding between wetlands may be due to the smaller GIWs having a greater influence on quick-flow events and vegetation cover mitigating excessive runoff and controlling water table levels. Hydrological processes in wetlands are controlled by a combination of climate and hydrogeomorphology factors. The regime of precipitation and geological structure plays a significant role in wetland hydroperiods, contributing to the accumulation of water. The GIWs' topographic position is important for catchment hydrology as they serve as recharge points and maintain groundwater for discharge areas, influencing the local and regional hydrological cycles.

Conclusions

The hydrodynamics study of the wetlands in the Paulista Peripheral Depression is crucial, especially considering their location at the interface between the Atlantic Forest and Cerrado ecosystems, which are significant agricultural and environmental frontiers in Brazil. This study utilizes various remote sensing, geophysical, and climatological techniques to consolidate data on these ecosystems. The classification of these areas as geographically isolated wetlands (GIWs) contributes to the development of national legislation and supports better management practices and governance.

Satellite data analysis is valuable for studying historical trends of GIWs. However, due to the small size of these ecosystems, there was an observed discrepancy of approximately 13% between satellite measurements and UAV datasets. The integration of seasonal, high-resolution UAV imaging with climatological data has advanced our understanding of the complex dynamics of surface water in GIWs. Additionally, the use of electrical resistivity tomography (ERT) confirmed the interaction between surface water, soil water, and groundwater in the central areas of GIWs, emphasizing their ecological and social importance.

Acknowledgments

The authors are especially grateful to the Fundação de Amparo à Pesquisa do Estado de São Paulo (Process n. 2020/03207-9) for funding the project and to the Center for Environmental Analysis and Planning (CEAPLA, Unesp) for providing climatological data. We would also like to thank the Coordenação de Aperfeiçoamento de Pessoal de Nível Superior (CAPES) for financial support on the PhD scholarships of L.M.F. and M.F.S.C.

References

ABEM, 2012. Terrameter LS—Instruction manual. ABEM Instrument, Sundbyberg, Sweden.

DJI. Phantom 4PRO. Available online: https://www.dji.com/br/phantom-4-pro (accessed on 30 November 2022).

Fries, A.; Silva, K.; Pucha-Cofrep, F.; Oñate-Valdivieso, F.; Ochoa-Cueva, P. Water balance and soil moisture deficit of different vegetation units under semiarid conditions in the andes of southern Ecuador. *Climate* 2020, 8(2), 30. https://doi.org/10.3390/cli8020030.

Instituto Nacional de Pesquisas Espaciais. Available online: http://www.dgi.inpe.br/catalogo/ (accessed on 2019-2020).

Kandus, P.; Minotti, P. G.; Morandeira, N. S.; Grimson, R.; González Trilla, G.; González, E. B., ... Gayol, M. P. Remote sensing of wetlands in South America: status and challenges. *Int. J. Remote Sens.* 2018, 39(4), 993-1016. https://doi.org/10.1080/01431161.2017.1395971

Kearey P.; Brooks M.; Hill I. *An introduction to geophysical exploration*. Tradução de Maria Cristina Moreira Coelho, 1st edition, Oficina de Textos, 2002, São Paulo. Portuguese.

Milson J. *Field geophysics*. 2003, Wiley, England

Mitsch, W. J.; Gosselink, J. G. The value of wetlands: importance of scale and landscape setting. *Ecol. Econ.* 2000, 35:25-33.

Moreira, C.A.; Rosolen, V.; Furlan, L.M.; Bovi, R.; Masquelin, H. Hydraulic conductivity and geophysics (ERT) to assess the aquifer recharge capacity of an inland wetland in the Brazilian Savanna. *Environ. Chall.* 2021, 5, 100274.

Mousa, Y. A.; Hasan, A. F.; Helmholz, P. Spatio-Temporal Analysis of Sawa Lake's Physical Parameters between (1985–2020) and Drought Investigations Using Landsat Imageries. *Remote Sens*. 2022, 14(8), 1831.

PIX4D. Available online: ttps://www.pix4d.com/ (accessed on 30 November 2022).

Rubin, Y.; Hubbard, S.J. *Hydrogeophysics*. 2006. Dordrecht:Springer.

USGS Earth Explorer. Available in: https://earthexplorer.usgs.gov/ (accessed on 2019-2020).